VIP Monomeric Phosphazenes

DOI: 10.1002/ange.200901380

Difluoro-λ^5-Phosphinonitrile $F_2P{\equiv}N$: Matrix Isolation and Photoisomerization into FP=NF**

*Xiaoqing Zeng, Helmut Beckers, and Helge Willner**

Oligomeric phosphazenes with repeating units $[\text{-}NPX_2\text{-}]_n$ have found a wide range of applications in medicine, conducting polymers, elastomers, membranes, lubricants, additives etc.[1,2] Their corresponding monomers, X_2PN (nitridophosphines, phosphinonitriles), first generated as intermediates about 25 years ago by photolysis of phosphinyl azides, X_2PN_3 [Eq. (1)],[3] have emerged as building blocks in synthetic organophosphorus chemistry.[4]

$$X_2PN_3 \rightarrow X_2PN\ (^1A_1) + N_2 \qquad (1)$$

Photolysis or thermolysis of organic azides usually forms nitrenes, R–N, having a triplet ground state.[5] However, the presence of an electron lone pair at the phosphorus atom [Eq. (2)] stabilizes a P=N bond and a singlet ground state. The

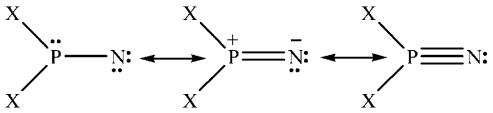

(2)

phosphorus derivatives X_2PN can thus be regarded as nitrido-λ^5-phosphines **2** rather than λ^3-phosphinonitrenes **1**.[4] Furthermore, these derivatives are more commonly referred to as λ^5-phosphinonitriles **3** in the literature, which, for convenience, is also assumed here.

λ^5-Phosphinonitriles undergo polymerization or 1,2-addition reactions with trapping reagents rather than the typical insertion reactions of nitrenes.[4] The P=N bond also significantly raises the barrier for unimolecular Curtius-like rearrangements according to Equation (3).[6,7]

$$X_2PN\ (^1A_1) \rightarrow XP{=}NX\ (^1A') \qquad (3)$$

Despite the long history of λ^5-phosphinonitriles, no unambiguous spectroscopic evidence has yet been obtained for their existence. This may be explained by their inherent instability. Recent ab initio calculations have shown that X_2PN is in fact less stable than the rearranged imino-λ^3-phosphines, XP=NX for X = H[7] and CH_3.[6] However, the relative stability between these two isomers dramatically depends on the nature of the substituent X.

For X = F we have calculated the geometries and relative energies of all possible species along the pathways of the thermal isomerization of F_2PN at both the density functional theory (DFT)[8] B3LYP[9] and BP86,[10] and the ab initio second-order Møller–Plesset perturbation (MP2)[11] levels using the 6-311 + G(3df) basis set.[12,13] The predicted relative energies and geometries of singlet and triplet F_2PN, *cis*- and *trans*-FP=NF, and of the singlet transition states of the 1,2-fluorine shift (TS1), and the *cis*--*trans* isomerization of the FP=NF isomers (TS2) are given in Figures S1 and S2, and Tables S1–S3 in the Supporting Information. The relative energies of the F_2PN isomers are similar to the values obtained previously at different levels of ab initio theory using smaller basis sets.[14] Although the estimated energies vary between the DFT and ab initio MP2 methods, the relative stabilities of the F_2PN isomers remain the same. Those predicted at the DFT B3LYP/6-311 + G(3df) level are shown in Figure 1. The planar singlet F_2PN is the global minimum.

The fact that the relative stabilities of $X_2PN > XP{=}NX$ with X = F are reversed compared to that with X = H, CH_3 can primarily be attributed to the significant difference in bond energies of the two bonds[15] involved: P–F (544 kJ mol^{-1})[16] > N–F (278 kJ mol^{-1}).[17] Both the rather high singlet–triplet energy gap (58.6 kJ mol^{-1}) and the high barrier (229.3 kJ mol^{-1}) for the 1,2-fluorine shift to *trans*-FP=NF are in accord with structure **2** in Equation (2). Of the two FP=NF isomers, the *trans* isomer is predicted at the DFT B3LYP level to be higher in energy by 10.7 kJ mol^{-1} than the *cis* isomer, and separated from the latter by a nitrogen-inversion barrier of only 66.4 kJ mol^{-1}.

Because of its remarkable stability (but possible high reactivity), F_2PN constitutes an attractive candidate for a matrix isolation study. To facilitate experimental assignments, the infrared fundamental frequencies, their intensities, and $^{14}N/^{15}N$ isotopic shifts were calculated for singlet/triplet F_2PN and *cis*/*trans*-FP=NF at the DFT and MP2 levels of theory. The complete list of the calculated vibrational data is collected in Tables S4 and S5 in the Supporting Information. Since the calculations on similar known molecules (NF_3 and PF_3, Tables S6 and S7 in the Supporting Information) showed that the MP2/6-311 + G(3df) results agreed slightly better with the experimental data, we have chosen this method for

[*] Dr. X. Zeng, Dr. H. Beckers, Prof. Dr. H. Willner
FB C – Mathematik und Naturwissenschaften, Fachgruppe Chemie
Bergische Universität Wuppertal
Gaußstrasse 20, 42097 Wuppertal (Germany)
Fax: (+49) 202-439-3053
E-mail: willner@uni-wuppertal.de

[**] This work was supported by the Deutsche Forschungsgemeinschaft and the Fonds der Chemischen Industrie. X.Z. acknowledges a fellowship from the Alexander von Humboldt Foundation. We are indebted to T. Benter and his group for providing the ArF excimer laser.

Supporting information for this article is available on the WWW under http://dx.doi.org/10.1002/anie.200901380.

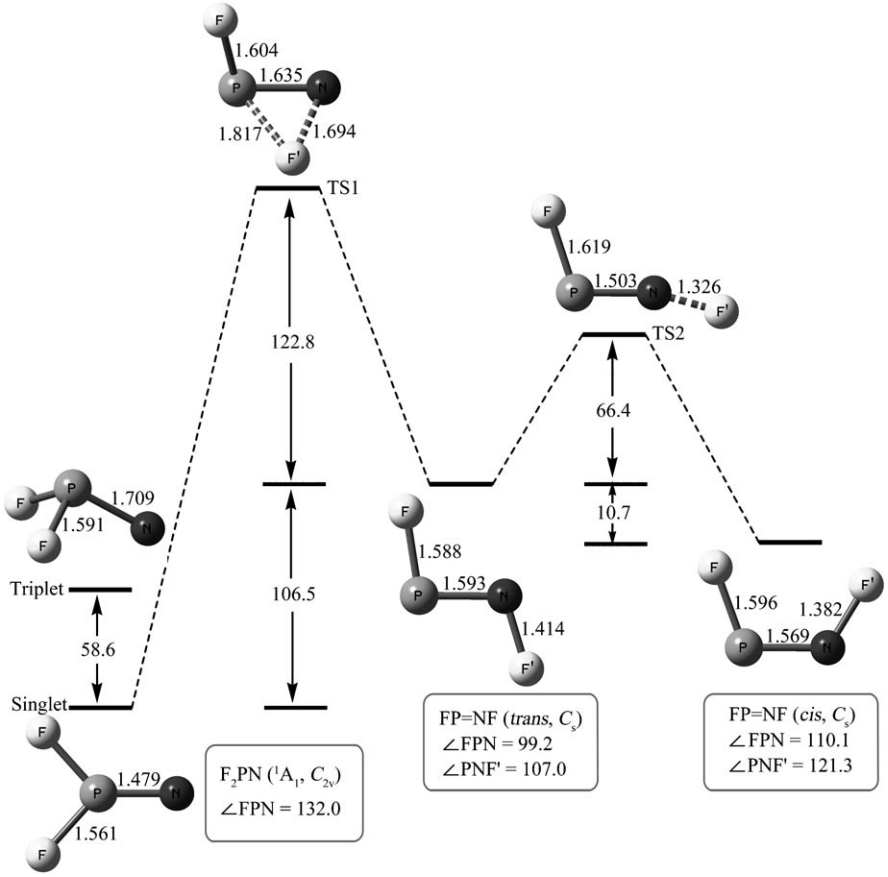

Figure 1. Selected distances [Å], angles [°], and relative energies [kJ mol^{-1}] of singlet and triplet F_2PN, *cis*- and *trans*-FP=NF, and of the transition states TS1 and TS2 of the pathways for the thermal isomerization of the singlet F_2PN species at the DFT B3LYP/6-311+G(3df) level of theory.

the calculations of singlet/triplet F_2PN and *cis*/*trans*-FP=NF; the vibrational data are listed in Tables 1 and 2, respectively.

F_2PN was synthesized from the matrix-isolated azide F_2PN_3 at 16 K by irradation with an ArF excimer laser (193 nm). The IR absorptions of the azide decreased and six new bands appeared with increasing photolysis time. In the difference spectrum shown in Figure 2, bands with decreasing transmittance indicate the formation of new products, whereas those with increasing transmittance indicate depletion of the precursor. The positions and relative intensities of the six new product bands agree very well with those predicted for F_2PN (Table 1). Subsequent photolysis of F_2PN by irradiation with a high-pressure mercury arc lamp ($\lambda = 255$ nm) depleted the F_2PN bands and new bands appeared (Figure 3). These new bands are attributed to *cis*-FP=NF by comparison with the calculated values in Table 2.

The assignments of the new IR bands in Figures 2 and 3 were confirmed by additional experiments using an equimolar mixture of $F_2P^{15}NNN$ and $F_2PNN^{15}N$ in place of F_2PN_3. Nearly all product bands split into 1:1 doublets and both components reveal the same matrix site band pattern (Figures S3 and S4 in the Supporting Information). The isotopic pattern proves that the novel species contain one N atom. Furthermore all observed $^{14}N/^{15}N$ isotopic shifts are very close to those predicted for F_2PN ($^1A_1$) and *cis*-FP=NF as listed in Tables 1 and 2, respectively. While the thermal rearrangement of singlet F_2PN is predicted to proceed by the initial formation of *trans*-FP=NF (Figure 1), surprisingly only the *cis* isomer was observed in our experiments.

To study the reactivity of F_2PN ($^1A_1$), F_2PN_3 was isolated in a solid CO matrix, irradiation ($\lambda = 193$ nm) of the CO matrix yielded new IR absorptions at 2287 (m), 2271 (vs), 846 (s), 826 (s), 707 (m), 612 (m), and 595 cm^{-1} (m). By comparison with the Ar matrix IR data of an authentic sample of F_2PNCO (2297 (m), 2274 (vs), 858 (s), 839 (s), 705 (m), 611 (m), and 597 cm^{-1} (m)), this isocyanate was unequivocally identified as the sole photolysis product [Eq. (4)]. This result clearly demonstrates, that the photo-decomposition ($\lambda = 193$ nm) of F_2PN_3 proceeds through the reactive singlet F_2PN intermediate, which in the absence of trapping agent, undergoes 1,2-fluorine shift to *cis*-FP=NF under UV irradiation ($\lambda =$ 255 nm).

$$F_2PN\ (^1A_1) + CO \rightarrow F_2PNCO \qquad (4)$$

The most prominent feature observed for F_2PN is the PN stretching vibration at 1372.0 cm^{-1} exhibiting a large $^{14}N/^{15}N$ isotopic shift of 24.4 cm^{-1}. This wavenumber is close to those of the SiO and SC stretches of the isoelectronic species $F_2Si{=}O$ 1309 cm^{-1} [18] and $F_2C{=}S$ 1368 cm^{-1},[19] respectively, and even higher than the PN stretch of

Table 1: Experimental band positions [cm^{-1}], $^{14}N/^{15}N$ isotopic shifts [cm^{-1}], and assignments for singlet F_2PN are compared with calculated IR data for singlet and triplet F_2PN.

Experimental Ar matrix: $F_2P^{14}N$			Calculated: $F_2P^{14}N$[c]			
			singlet		triplet	
ν_i[a]	$\Delta\nu_i(^{14}N/^{15}N)$[b]	assignment	ν_i	$\Delta\nu_i(^{14}N/^{15}N)$[b]	ν_i	$\Delta\nu_i(^{14}N/^{15}N)$[b]
1372.0 (28)	24.4	$\nu_1(A_1)$	1388.6 (57)	25.4	845.8 (142)	0.0
898.2 (100)	0.0	$\nu_4(B_2)$	884.7 (178)	0.0	842.4 (175)	0.0
815.6 (64)	6.1	$\nu_2(A_1)$	807.2 (117)	6.1	739.7 (15)	17.5
424.3 (7)	1.1	$\nu_3(A_1)$	422.9 (21)	1.1	398.6 (34)	1.6
315.9 (6)	5.1	$\nu_5(B_1)$	342.7 (22)	2.7	310.6 (6)	2.7
250.6 (11)	1.3	$\nu_6(B_2)$	295.4 (10)	4.7	289.3 (10)	4.4

[a] Most intensive matrix site; relative integrated intensities [%] in parenthesis. [b] Isotopic shifts of $F_2P^{15}N$ relative to $F_2P^{14}N$. [c] MP2/6-311+G(3df) level of theory with absolute intensities [km mol^{-1}] in parenthesis.

Table 2: Experimental band positions [cm^{-1}], $^{14}N/^{15}N$ isotopic shifts [cm^{-1}], and assignments for *cis*-FP=NF are compared with calculated IR data for *cis*- and *trans*-FP=NF.

Experimental Ar matrix: $FP^{14}NF$			Calculated: $FP^{14}NF$[c]			
		assignment	*cis*		*trans*	
ν_i[a]	$\Delta\nu_i(^{14}N/^{15}N)$[b]		ν_i	$\Delta\nu_i(^{14}N/^{15}N)$[b]	ν_i	$\Delta\nu_i(^{14}N/^{15}N)$[b]
1116.8 (19)	25.3	ν_1(A′)	1179.2 (31)	28.7	1064.9 (9)	25.2
826.5 (100)	0.7	ν_2(A′)	825.9 (169)	2.1	905.9 (150)	11.1
795.2 (39)	11.8	ν_3(A′)	807.8 (56)	10.2	847.2 (75)	4.8
517.7 (12)	5.8	ν_4(A′)	519.7 (17)	6.7	414.5 (6)	2.6
351.3 (11)	6.6	ν_5(A″)	368.2 (13)	7.0	269.5 (0.3)	3.9
		ν_6(A′)	150.6 (4)	0.2	219.7 (4)	1.3

[a] Most intensive matrix site; relative integrated intensities [%] in parenthesis. [b] Isotopic shifts of $FP^{15}NF$ relative to $FP^{14}NF$. [c] At MP2/6-311 + G(3df) level of theory with absolute intensities [km mol^{-1}] in parenthesis.

to the PN stretch because of its large $^{14}N/^{15}N$ shift ($\Delta\nu(^{14}N/^{15}N) = 25.3\ cm^{-1}$). The strong PF stretch at 826.5 cm^{-1} is close to that of the similar molecule FP=O (gas phase: 819.6 cm^{-1} [22]). The band at 795.2 cm^{-1} showing an isotopic shift of 11.8 cm^{-1} is assigned to the NF stretch.

The higher PN stretching frequency of *cis*-FP=NF can be explained by a lone-pair-related n(N)→σ*(PF) hyperconjugation,[23] a similar lone-pair delocalization may also account for the high PN stretching frequency observed for F_2PN (1372.0 cm^{-1}). The calculated DFT (B3LYP/6-311 + G(3df)) bond lengths, force constants, and Wiberg bond indices (WBI)[24] of F_2PN (148 pm, 21.3 N cm^{-1}, 2.43) and of diatomic P≡N (148 pm, 19.7 N cm^{-1}, 2.73) are very similar, indicating a triple bond for singlet F_2PN. Small differences between these bond parameters may be explained by the higher polarity of the PN bond in F_2PN.

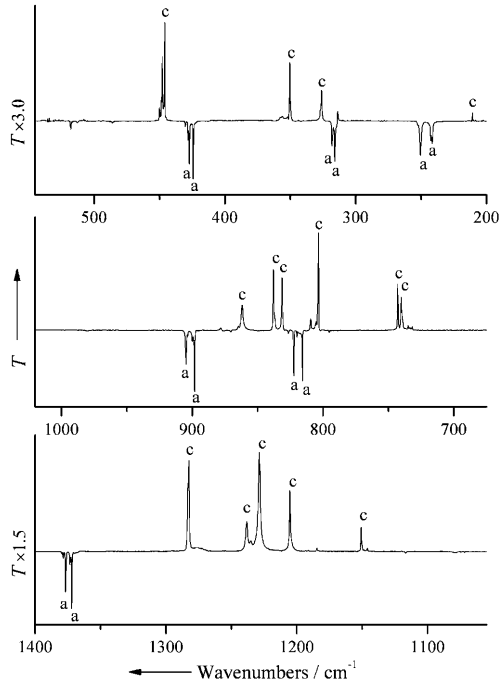

Figure 2. Difference IR spectra obtained by subtracting the IR spectrum of Ar-matrix-isolated F_2PN_3 recorded before and after irradation with an ArF excimer laser ($\lambda = 193$ nm). Bands associated with singlet F_2PN and F_2PN_3 are denoted by a and c, respectively.

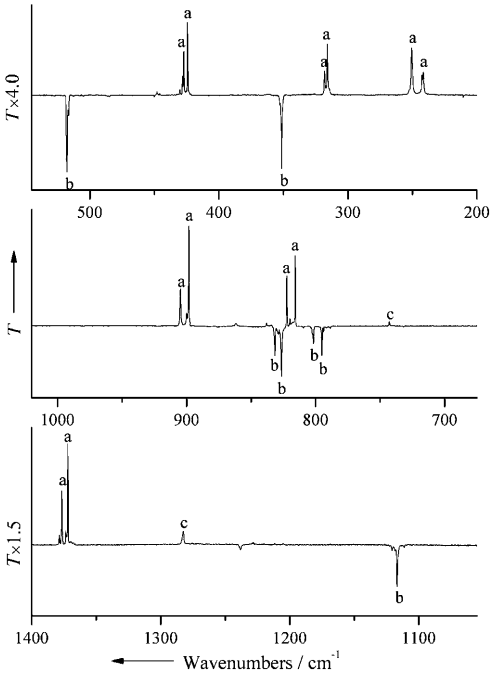

Figure 3. Difference IR spectra obtained by subtracting the IR spectrum of Ar-matrix-isolated F_2PN_3/F_2PN recorded before and after irradiation with a high-pressure mercury arc lamp ($\lambda = 255$ nm). Bands associated with singlet F_2PN, *cis*-FP=NF, and F_2PN_3 are denoted by a, b, and c, respectively.

the diatomic P≡N (gas phase 1337 cm^{-1},[20] Kr matrix 1323 cm^{-1} [21]). The wavenumber of the PN stretch of F_2PN is clearly consistent with a P=N bond of a planar tricoordinated λ^5-phosphinonitrile. The PF_2 stretches appear at 898.2 and 815.6 cm^{-1}. As a result of stronger vibrational coupling they are more separated than those usually observed in λ^3-phosphines like F_2PN_3 (861.8 and 837.8 cm^{-1}, Figure 2). The PF_2 bending and the out-of-plane deformations of singlet F_2PN at 424.3 and 315.9 cm^{-1} are both similar with the corresponding deformations of F_2SiO (423 and 344 cm^{-1}). The PF_2 rocking of F_2PN is assigned to a weak band at 250.6 cm^{-1}.

The two geometric FP=NF isomers are calculated to have considerable different vibrational frequencies (Table 2). The highest fundamental of *cis*-FP=NF at 1116.8 cm^{-1} is assigned

Experimental Section

Caution! Difluoro(azido)phosphine F_2PN_3 is potentially explosive. It should be prepared in less than millimolar quantities, and safety

precautions must be taken when it is manipulated in the liquid or solid state.

Difluoro(azido)phosphine F_2PN_3[25] and difluoro(isocyanato)-phosphine F_2PNCO[26] were prepared according to literature procedures and purified by repeated fractional condensation in vacuum. For the preparation of ^{15}N-labeled F_2PN_3, 1-^{15}N sodium azide (98 atom% ^{15}N, EURISO-TOP GmbH) was used. The purity of F_2PN_3 was checked by spectroscopic characterization. ^{19}F NMR (235.3 MHz, CD_2Cl_2, RT): $\delta = -57.8$ ppm (d, $J(P,F) = 1309$ Hz); ^{31}P NMR (101.2 MHz, CD_2Cl_2, RT): $\delta = 149.1$ ppm (t); FTIR (gas, 6 mbar, RT): $\tilde{\nu} = 2154$ (vs), 1267 (s), 1231 (s), 856 (s), 839 (s, br), 743 (s), 611 (s), 560 (w), 447 cm^{-1} (w); UV/Vis (gas, 3 mbar): $\lambda_{max} = 205$ (s), 245 nm (sh). FTIR spectrum of ^{15}N-labeled F_2PN_3 (gas, 6 mbar, RT): $\tilde{\nu} = 2137$ (vs), 1239 (s), 1204 (s), 856 (s), 839 (s, br), 734 (s), 609 (s), 559 (w), 446 cm^{-1} (w); FT-IR spectrum of F_2PNCO (gas, 6 mbar, RT): $\tilde{\nu} = 2394$ (m), 2281 (vvs), 1436 (m), 1405 (m), 852 (vs, br), 718 (s), 608 (s), 443 cm^{-1} (w).

Spectroscopic investigations: IR spectra of the matrix-isolated species were recorded on an FTIR spectrometer (IFS 66v/S Brucker) in reflectance mode using a transfer optic. A KBr beam splitter and a MCT detector were used in the region of 5000–530 cm^{-1} and a Ge-coated 6-μm Mylar beam splitter with liquid-helium-cooled Si bolometer was used in the region of 700–150 cm^{-1}. For each spectrum 200 scans at a resolution of 0.25 cm^{-1} were coadded.

Preparation of the matrices: The stable gaseous precursor F_2PN_3 was mixed with argon (1:500) in a 1 L stainless-steel storage container, and then small amounts (ca. 1 mmol) of the mixture were deposited within 30 min onto the cold matrix support (16 K, Rh-plated Cu block) in high vacuum. Photolysis experiments were carried out with an ArF excimer laser (Lambda-Physik, 2 mJ, 20 min) and a high-pressure mercury arc lamp (TQ 150, Heraeus). The latter source was used in combination with a water-cooled quartz lense and an interference filter (255 nm, Schott) for 50 min. Details of the matrix apparatus have been described elsewhere.[27]

Theoretical calculations: Quantum chemical calculations were carried out using the Gaussian 03 software package.[28] The 6-311 + G(3df) basis set[12] was used for all calculations. The geometries of all stationary points were fully optimized with ab initio (MP2,[11] CBS-QB3[29]) and DFT[8] (B3LYP,[9] BP86[10]) methods. Local minima were confirmed by vibrational frequency analysis, and transition states were further confirmed by intrinsic reaction coordinate (IRC)[30,31] calculations. Spin-unrestricted methods were utilized for the calculations of the triplet species. Natural bond order (NBO)[32] analysis was performed using NBO 3.1 implemented in Gaussian 03 with the B3LYP method.

Received: March 12, 2009
Published online: May 26, 2009

Keywords: IR spectroscopy · matrix isolation · phosphazenes · photoisomerization

[1] H. R. Allcock, *Curr. Opin. Solid State Mater. Sci.* **2006**, *10*, 231 – 240.
[2] H. R. Allcock in *Synthesis and Characterisations of Poly(organophosphazenes)* (Eds.: M. Gleria, R. De Jaeger), Nova Science, New York, **2004**, pp. 1 – 22.
[3] G. Sicard, A. Baceiredo, G. Bertrand, J.-P. Majoral, *Angew. Chem.* **1984**, *96*, 450 – 451; *Angew. Chem. Int. Ed. Engl.* **1984**, *23*, 459 – 460.
[4] J.-P. Majoral in *Multiple Bonds and Low Coordination in Phosphorus Chemistry* (Ed.: M. Regitz), Georg Thieme, Stuttgart, **1990**, pp. 455 – 461.
[5] M. S. Platz, in *Reactive Intermediate Chemistry* (Eds.: R. A. Moss, M. S. Platz, M. Jones, Jr.), Wiley, New York, **2004**, pp. 501 – 559.
[6] R. D. McCulla, G. A. Gohar, C. M. Hadad, M. S. Platz, *J. Org. Chem.* **2007**, *72*, 9426 – 9438.
[7] C.-H. Lai, M.-D. Su, S.-Y. Chu, *J. Phys. Chem. A* **2003**, *107*, 2700 – 2710.
[8] R. G. Parr, W. Yang in *Density-Functional Theory of Atoms and Molecules*, Academic Press, London, **1994**.
[9] A. D. Becke, *J. Chem. Phys.* **1993**, *98*, 5648.
[10] J. P. Perdew, *Phys. Rev. B* **1986**, *33*, 8822 – 8824.
[11] C. Møller, M. S. Plesset, *Phys. Rev.* **1934**, *46*, 618 – 622.
[12] R. Krishnan, J. S. Binkley, R. Seeger, J. A. Pople, *J. Chem. Phys.* **1980**, *72*, 650 – 654.
[13] To verify the theoretical methods we used, additional calculations on NF_3 and PF_3 were carried out. The results are included in the Supporting Information. For these two species the B3LYP and MP2 methods present better agreement with the experimental results than BP86.
[14] M. T. Nguyen, H. Vansweevelt, T.-K. Ha, L. G. Vanquickenborne, *J. Chem. Soc. Chem. Commun.* **1990**, 1425 – 1427.
[15] Experimental values of the first bond dissociation energies of PF_3 and NF_3 are used for convenience.
[16] D. J. Grant, M. Matus, H. , J. Switzer, R. , D. A. Dixon, J. S. Francisco, K. O. Christe, *J. Phys. Chem. A* **2008**, *112*, 3145 – 3156.
[17] W. D. Good, N. K. Smith, *J. Chem. Eng. Data* **1970**, *15*, 147 – 150.
[18] H. G. Schnöckel, *J. Mol. Struct.* **1980**, *65*, 115 – 123.
[19] A. J. Downs, *Spectrochim. Acta* **1963**, *19*, 1165 – 1171.
[20] K. P. Huber, G. Hertzberg, *Molecular Spectra and Molecular Structure. IV Constants of Diatomic Molecules*, Van Nostrand Reinhold, New York, **1979**, p. 536.
[21] R. M. Atkins, P. L. Timms, *Spectrochim. Acta Part A* **1977**, *33*, 853 – 857.
[22] H. Beckers, H. Buerger, P. Paplewski, M. Bogey, J. Demaison, P. Drean, A. Walters, J. Breidung, W. Thiel, *Phys. Chem. Chem. Phys.* **2001**, *3*, 4247 – 4257.
[23] T. Yamamoto, D. Kaneno, S. Tomoda, *J. Org. Chem.* **2008**, *73*, 5429 – 5435.
[24] K. B. Wiberg, *Tetrahedron* **1968**, *24*, 1083 – 1096.
[25] S. R. O'Neil, J. M. Shreeve, *Inorg. Chem.* **1972**, *11*, 1629 – 1631.
[26] G. G. Flaskerud, K. E. Pullen, J. M. Shreeve, *Inorg. Chem.* **1969**, *8*, 728 – 730.
[27] H. G. Schnöckel, H. Willner, in *Infrared and Raman Spectroscopy, Methods and Applications* (Ed.: B. Schrader), VCH, Weinheim, **1994**.
[28] Gaussian 03 (Revision B.05): M. J. Frisch et al., see the Supporting Information.
[29] J. A. Montgomery, Jr., M. J. Frisch, J. W. Ochterski, G. A. Petersson, *J. Chem. Phys.* **2000**, *112*, 6532 – 6542.
[30] C. Gonzalez, H. B. Schlegel, *J. Chem. Phys.* **1989**, *90*, 2154 – 2161.
[31] C. Gonzalez, H. B. Schlegel, *J. Phys. Chem.* **1990**, *94*, 5523 – 5527.
[32] A. E. Reed, L. A. Curtiss, F. Weinhold, *Chem. Rev.* **1988**, *88*, 899 – 926.

